Ge_2Pt hut clusters: A substrate for germanene

Rik van Bremen,[1,2,a)] Pantelis Bampoulis,[1,2,3] Johannes Aprojanz,[3,4] Mark Smithers,[2] Bene Poelsema,[1,2] Christoph Tegenkamp,[3,4] and Harold J. W. Zandvliet[1,2]
[1]*Physics of Interfaces and Nanomaterials, University of Twente, P.O. Box 217, 7500 AE, Enschede, The Netherlands*
[2]*MESA+ Institute for Nanotechnology, Hallenweg 15, 7522 NB, Enschede, The Netherlands*
[3]*Institut für Festkörperphysik, Leibniz Universität Hannover, Appelstraße 2, 30167, Hannover, Germany*
[4]*Institut für Physik, Technische Universität Chemnitz, Reichenhainer Str. 70, 09126, Chemnitz, Germany*

(Received 4 July 2018; accepted 31 August 2018; published online 25 September 2018)

The formation and structure of Ge_2Pt clusters was studied in order to understand their germanene termination layer. The Ge_2Pt clusters are formed by depositing a few layers of Pt on a Ge(110) surface. Annealing at temperatures above 1043 K results in eutectic Ge-Pt droplets that etch grooves on the surface in the $[1\bar{1}0]$ direction. Upon cooling down, they solidify and decompose into a Ge_2Pt phase and a pure Ge phase. Electron diffraction reveals that the hut-shaped clusters have their (001) plane oriented parallel to the Ge(110) surface and their (100) plane facing in the Ge$[1\bar{1}0]$ direction. The facets of the Ge_2Pt hut clusters have been determined to be the {101} and {011} planes. The germanene layers which cover these facets are commensurate with the {101} and {011} facets of the Ge_2Pt substrate. *Published by AIP Publishing.* https://doi.org/10.1063/1.5046997

I. INTRODUCTION

Germanene is a 2D material analogous to graphene. The germanium atoms in germanene form a buckled honeycomb lattice.[1] The two hexagonal sub-lattices in low-buckled free-standing germanene are predicted to be vertically displaced from each other by 0.64 Å[2] and have a lattice constant of 4.1 Å.[3] The charge carriers in germanene behave as Dirac fermions with a predicted Fermi velocity of 3.8×10^5 m/s.[4] The advantage of germanene over graphene is that germanene has a substantial spin-orbit gap of 23.9 meV.[5] This allows germanene to exhibit the quantum spin Hall effect at temperatures that are easily accessible.[5,6] In addition, owing to the buckling of germanene, it is relatively easy to open a bandgap, making germanene an ideal material for a 2D field effect transistor.[6–9]

Germanene has been grown on several substrates such as Pt(111),[10] Au(111),[11] Al(111),[12] MoS_2,[13] and Ge_2Pt clusters.[14] The germanene on Ge_2Pt system is probably best documented. In this system, both the honeycomb lattice of germanene was directly imaged[14] and the linear density of states, which is characteristic of Dirac materials, was confirmed.[15]

A disadvantage of the germanene growth on Ge_2Pt clusters is that the size of the sheets is limited by the size of the clusters. Generally, the clusters are only a few hundred nanometers in size. To increase the size of these germanene sheets, either the size of the clusters needs to be increased or the germanene needs to be grown on a suitable bulk Ge_2Pt substrate.

Another disadvantage of the system is that the growth process of the Ge_2Pt clusters and the details of the formation of germanene are still unknown. In previous works,[14,15] the Ge_2Pt clusters were grown by depositing Pt on Ge(110) at room temperature followed by annealing at temperatures exceeding 1043 K. The clusters were already proposed to consist of Ge_2Pt, because in the bulk phase diagram, the eutectic phase will decompose in a pure Ge phase and a Ge_2Pt phase upon solidification. In a later study, $MoSi_2$ clusters were grown on Si using the same method.[16] These $MoSi_2$ clusters also exhibit a honeycomb lattice which the authors attributed to be a silicene layer.[16] Similar to the Ge_2Pt system, the role of the clusters as substrate was still not addressed. In both studies, the focus was on flat clusters, as small height variations are more suitable for scanning tunneling microscopy (STM) study.

In this article, we have characterized the Ge_2Pt clusters by combining scanning electron microscopy (SEM), electron backscatter diffraction (EBSD), and scanning probe microscopy (SPM) techniques. The most frequently occurring clusters have a very distinct hut shape. These Ge_2Pt clusters resemble very closely the well-studied hut clusters formed by Ge-epitaxy on Si(001).[17–20] We have carefully determined the crystal structure, the facets, and the interface with the Ge substrate of these hut shaped clusters. We found that the germanene layers grow on the {101} and {011} facets of the Ge_2Pt hut clusters. The oblique and rectangular lattices that are frequently found on the same facets are identified as the Pt atoms of the Ge_2Pt{101} planes. The germanene was found to be commensurate with the underlying substrate.

II. EXPERIMENTAL DETAILS

The Ge(110) substrate (from MTI Corporation) is cleaned by several cycles of Ar^+ ion bombardment followed by flash annealing in an ultrahigh vacuum (UHV) environment.[21] Subsequently, several layers of Pt are deposited on the germanium. Then, the sample is heated above its eutectic point of 1043 K. The eutectic phase is composed of 22 at. % Pt and 78 at. % Ge.[22] The temperature is kept well below the melting point of germanium. During heating, molten droplets of Ge-Pt move across the surface of the sample.[23] Upon

a)r.vanbremen@utwente.nl

cooling, the droplets solidify and form crystalline clusters on the surface. It has been proposed that upon cooling, the droplets undergo a decomposition into a Ge_2Pt phase and a pure Ge phase as deduced from the phase diagram.[23] Except for the STM measurements, the samples are exposed to ambient conditions when they are transferred to the different systems.

The secondary electron images were recorded in a Zeiss MERLIN HR-SEM with an HE-SE2 detector and an Omicron SEM system. The electron beam energy used was 15.0 keV. For the EBSD measurements, we have used an AZtec system from Oxford Instruments and a sample tilt angle of 70°.

An Agilent 5100 SPM was used for the atomic force microscopy (AFM) topography scans. The AFM was operated in tapping mode with a Hi'Res-C14/Cr-Au tip (from MikroMasch). The AFM measurements were performed in a nitrogen atmosphere.

STM data were obtained with a UHV Omicron low-temperature STM operated at 77 K. The tips used were made from an etched tungsten wire. Samples can be transferred from the preparation chamber to the STM chamber without breaking the vacuum.

The EBSD data are displayed using MTEX.[24] Crystal structure figures are produced using Vesta[25] and Jmol.[26] The scanning probe data were corrected and presented using Gwyddion.[27]

III. RESULTS AND DISCUSSION

A. Hut cluster characterization

After growth, different sizes and shapes of clusters can be found on the Ge(110) surface as seen in Fig. 1(a). The size and shape of the clusters differ per growth cycle and may depend on growth conditions such as annealing time, temperature, and amount of Pt deposition. Energy dispersive x-ray spectroscopy (EDX) provides information on the chemical composition of the clusters. On the cluster free regions, only germanium peaks

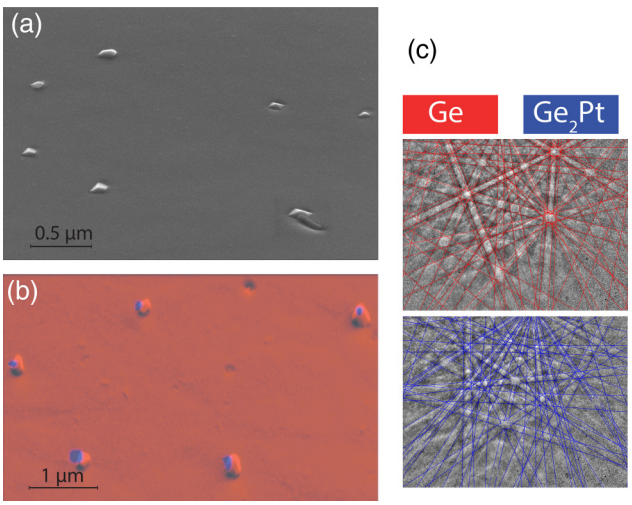

FIG. 1. (a) Secondary electron image of a selection of several clusters. (b) Another SEM image (after digital tilt correction) of several clusters with corresponding EBSD phase map. Away from the clusters, the diffraction pattern corresponds to pure germanium (red), while the clusters correspond to Ge_2Pt (blue). (c) Typical Kikuchi patterns from the substrate with a fit of the germanium model (red) and from a cluster with Ge_2Pt model (blue).

are detected, whereas all the Pt was found to be concentrated inside the clusters as shown in the supplementary material (Fig. 1). The exact ratio of the elements in the clusters cannot be determined, because a 15 keV electron beam energy was used which can easily penetrate through the relatively small clusters. For this reason, the Ge peak originating from the substrate is always significantly higher than the Pt peak.

We have used EBSD to determine the crystal structure of the clusters. We found that the clusters are composed of a Ge_2Pt alloy, as can be seen in Fig. 1(b). Representative diffraction patterns obtained from the clusters and the substrate are shown in Fig. 1(c). Different shapes of clusters were recorded, but all shapes have the same Ge_2Pt phase. The space group of Ge_2Pt is orthorhombic with lattice parameters 6.20 Å, 5.78 Å, and 2.91 Å.[28] The unit cell of this crystal structure is shown in the supplementary material (Fig. 2).

SEM and AFM images reveal a preference of the Ge_2Pt clusters for specific shapes. The most frequently occurring shape is shown in Fig. 2(a). We will refer to these clusters as Ge_2Pt hut clusters in analogy to the extensively studied Ge hut clusters grown on Si(001) that have a similar shape.[17–20] The Ge_2Pt hut clusters show numerous similarities to the Ge hut clusters. For instance, they are found in a wedge shaped version (with a rectangular base) and in a pyramidal shaped version (with a square base). Some of the clusters are flat-topped.[29] In addition, they are always aligned along two high-symmetry directions, just as the Ge hut clusters.[19] Some of the clusters have a "tail" as can be seen more clearly in the supplementary material (Fig. 3). This tail might be formed due to disposal of excess Ge during cooling down. No relation between growth parameters and the formation of a tail or flat-top has been found.

The property that the Ge_2Pt hut clusters always have the same shape and alignment on the surface makes them ideal clusters for characterization and allows us to find the crystal orientation of the clusters with respect to the substrate and determine their facets. Using EBSD, it is possible to determine the crystal orientation of both the substrate and the clusters. In Fig. 2(b), the EBSD result of such a hut cluster is shown. In the phase map, it can be seen that the Ge_2Pt hut cluster is clearly distinguishable from the substrate. The phase image is slightly shifted with respect to the gray-scale SEM image due to drift between making the SEM imaging and the EBSD measurement. The hut cluster looks slightly distorted in the SEM image, because it was originally imaged at an angle of 70° after which it has been digitally corrected. From the recorded Kikuchi patterns, the orientation of the Ge and Ge_2Pt crystals can be determined. These orientations are shown in the three inverse pole figure maps at the bottom of the figure. The color of the map indicates the crystallographic orientation as indicated by the corresponding Ge or Ge_2Pt legends. Each inverse pole figure map presents the orientation of both the substrate and the cluster in one of three directions: Z, X, or Y, which correspond to the directions indicated in the phase map. The Z direction is the direction perpendicular to the substrate. From the orientation maps, it can be seen that the crystal plane of the substrate that corresponds to this direction is the Ge(110) plane, as expected. For the cluster, this is the Ge_2Pt(001) plane. It should be noted that for the

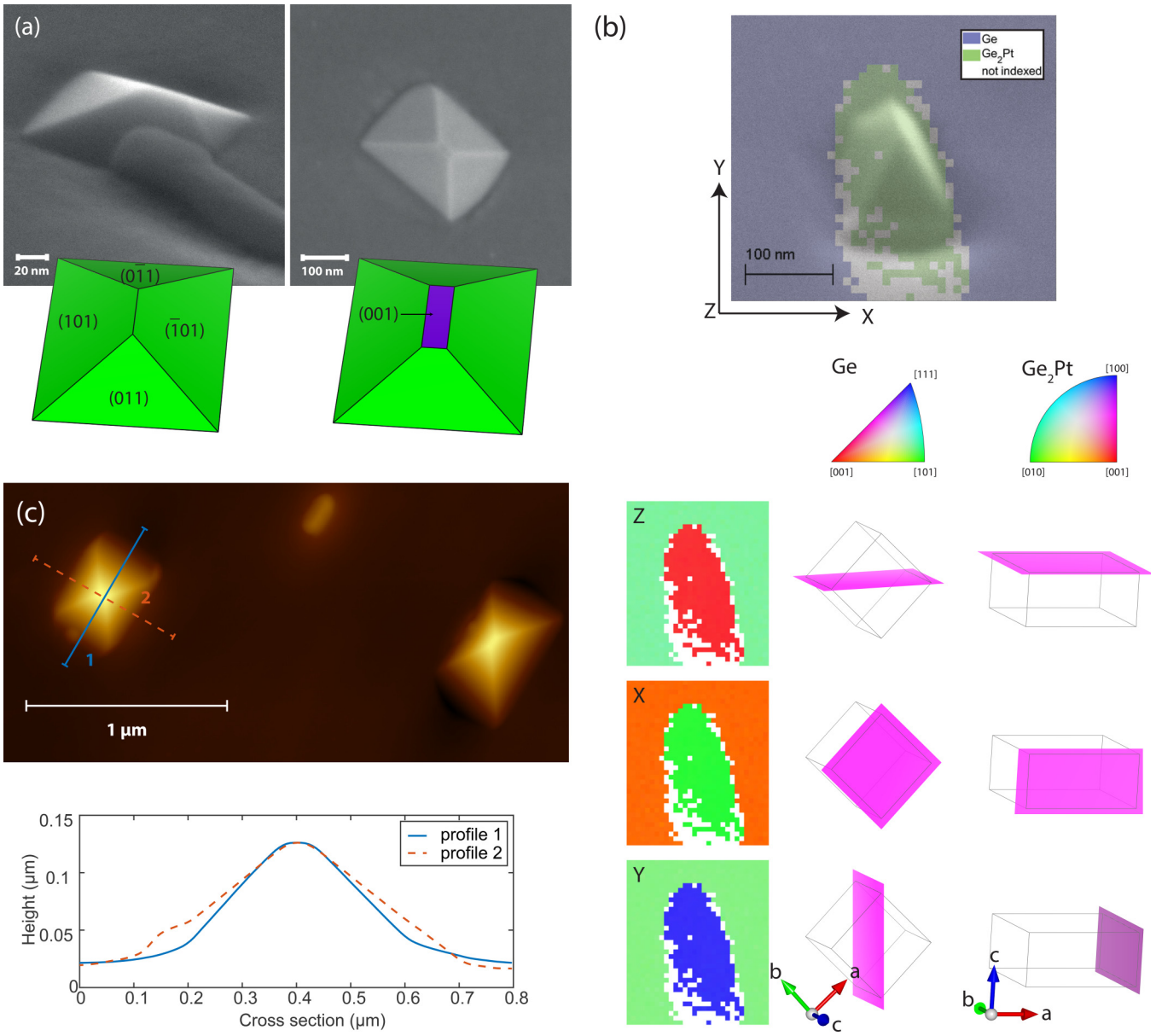

FIG. 2. (a) SEM images of two hut clusters. Two types are shown: a wedge and a flat-topped wedge. The 3D Wulff plots at the bottom show the {101} and {011} planes in green with a (001) flat-top plane in purple. (b) EBSD phase map of a hut cluster. The substrate is identified as Ge, the cluster as Ge_2Pt. The bottom half of the figure shows the inverse pole figure maps of the Ge and Ge_2Pt crystals. The color coding of the orientations is shown in the two legends. In the Z direction, the Ge(110) plane is parallel to the $Ge_2Pt(001)$ plane. In the X direction, the Ge(001) plane is parallel to the $Ge_2Pt(0\bar{1}0)$ plane. In the Y direction, the $Ge(1\bar{1}0)$ plane is parallel to the $Ge_2Pt(100)$ plane. (c) AFM topography image of two wedge-shaped clusters. By taking a cross section, the slope of the facets can be determined. Profile 1 has an average slope of 27° and profile 2 has an average slope of 21°.

Ge_2Pt crystal, the (100), (010), and (001) planes can be clearly distinguished from each other since the crystal structure is orthorhombic (in contrast to Ge, where all {100} planes are equivalent). The Y-direction corresponds to another Ge{110} plane of the substrate. From previous results, we know that this is the $Ge(1\bar{1}0)$ plane.[23] In the cluster, this corresponds to the $Ge_2Pt(100)$ plane. The X-direction corresponds to a Ge{100} plane of the substrate, which we know is the Ge(001) plane. This plane is parallel to the $Ge_2Pt(010)$ plane of the cluster.

Now, we can determine the planes of the Ge_2Pt clusters by beveling a bulk crystal which has the orientation as determined by the EBSD measurements. We measured the slope of the facets in AFM in order to find the angles of the appropriate planes. In Fig. 2(c), a topography image of two hut clusters is shown. By taking line profiles, the slope of the facets can be measured. The cross sections shown in the bottom part of the image correspond to the line profiles indicated by the red and blue lines. The slopes of the facets were found to be: 27° for profile 1 and 21° for profile 2. The close packed planes in the bulk Ge_2Pt crystal that closely match to the measured slopes are the {101} and {011} planes. These planes have a slope of 26.8° and 25.2°, respectively. The hut clusters have four facets and are thus terminated by two sets of {101} and {011} planes. There are two combinations of these planes that will result in a hut cluster. The first combination consists of the (011), (101), $(0\bar{1}1)$, and $(\bar{1}01)$ planes. The second combination comprises the $(0\bar{1}\bar{1})$, $(\bar{1}0\bar{1})$, $(01\bar{1})$, and

(10$\bar{1}$) planes. Using these planes, we can construct the corresponding 3D Wulff figure as shown in the insets of Fig. 2(a). Some of the hut clusters have a flat-top, as can be seen for the cluster in the right panel of Fig. 2(a). The flat top corresponds to a (001) plane.

Another important aspect of the cluster growth is the interface of the clusters with the substrate. For longer annealing times, elongated pits or grooves can be found on the surface as can be seen in the SEM image of Fig. 3(a). The inset shows that there are also smaller grooves. These grooves are well-known to form on the Ge(110) substrate during etching.[30,31] The grooves are a result of preferential etching during the annealing process. During annealing, liquid Ge-Pt droplets move parallel to the [1$\bar{1}$0] direction and dissolve Ge from the substrate. The droplets move in the [1$\bar{1}$0] direction, because this is the path with the lowest etch resistance.[30] After cooling, small clusters can be found at the most freshly etched part of the grooves, as seen in the inset. This indicates that all the droplets did move in the same direction. In a related study, the droplets were found to move in either of the two [1$\bar{1}$0] directions on a Si(110) surface.[32] The preferential movement direction in our experiments might possibly be determined by inhomogeneities on the surface, such as a temperature gradient[33] or a small mis-cut angle.[34].

The shape of the grooves is determined by preferential etching of Ge crystal planes. In previous studies, the {111}, {100}, and {110} planes were found to be the most stable facets against etching since these planes are the closest packed planes.[35,36] Previously, it was shown that the grooves etched by Ge-Au droplets in Ge(110) were terminated by Ge{111} and Ge {110} planes.[31] Similar results were obtained for etching of Si(110).[32] A similar process on our Ge(110) substrate with Pt would result in grooves in the Ge substrate with a shape as presented in the inset of Fig. 3(a). Often nanowires form in these grooves, making them invisible.[23,32] For Ge(100) samples, we found that the shape of the etched pits was square as can be seen in the supplementary material (Fig. 4). The shape of the square pits is defined by four {111} planes in agreement with previous work.[31]

In analogy to similar systems, we propose that the Ge_2Pt clusters nucleate and grow at the bottom of the grooves.[32,37] The growth of the clusters can be described in a few steps as schematically shown in Fig. 3(b). First, Pt is deposited on a clean Ge(110) substrate. Then during annealing, Ge-Pt droplets form on the substrate. These droplets will start to etch a groove in the substrate. The grooves have an elongated shape as shown before. Subsequently, upon cooling down to room temperature, the droplets nucleate and grow in these grooves, leaving behind a wedge shaped Ge_2Pt hut cluster. Due to the confinement in the pit, the clusters are also rectangular and are aligned along or perpendicular to the [1$\bar{1}$0] direction.[32]

The bottom of the grooves, at which the clusters grow, is the Ge(110) facet. From our previous EBSD results, we can determine the interface of the hut clusters which is parallel to the Ge(110) substrate. This is the (100) plane of the Ge_2Pt cluster. As mentioned earlier, the clusters have been found to always align along or perpendicular to the [1$\bar{1}$0] direction of the germanium substrate. This direction is the same direction as the zigzag rows of the bulk-terminated Ge(110) substrate.

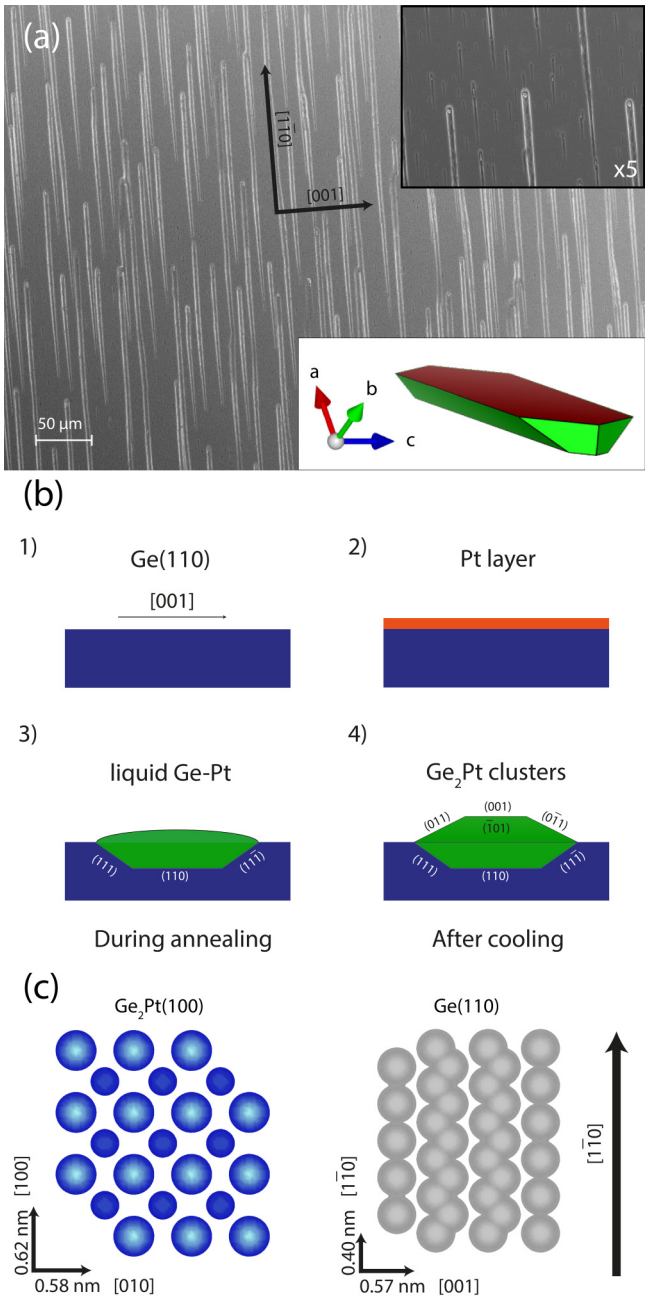

FIG. 3. (a) The hut pits are all aligned in the [1$\bar{1}$0] direction. The bottom inset shows the terminating Ge planes of the grooves. The {111} planes are colored green and the {110} planes are colored red. (b) Schematic presentation of the formation of the clusters. The view is along the [1$\bar{1}$0] direction. (c) The (001) plane of the Ge_2Pt clusters (only Pt atoms) interfaces with the Ge(110) substrate. Both are aligned in the vertical direction with the [1$\bar{1}$0] direction of the Ge(110) substrate.

The lattices of the Ge_2Pt(100) and the Ge(110) planes are schematically represented in Fig. 3(c). In the Ge_2Pt(100) plane, only the Pt atoms are displayed; the Ge atoms are omitted. Half of the Pt atoms lie in the plane, while the other half lie deeper, midway to the next lattice plane. These deeper lying atoms are indicated by smaller spheres in the figure. The lattice constants of the interface plane of the Ge_2Pt cluster are 0.62 nm and 0.58 nm.[28] The lattice constants of the Ge(110) substrate are 0.4 nm parallel to the zigzag rows and 0.57 nm perpendicular to the zigzag rows.

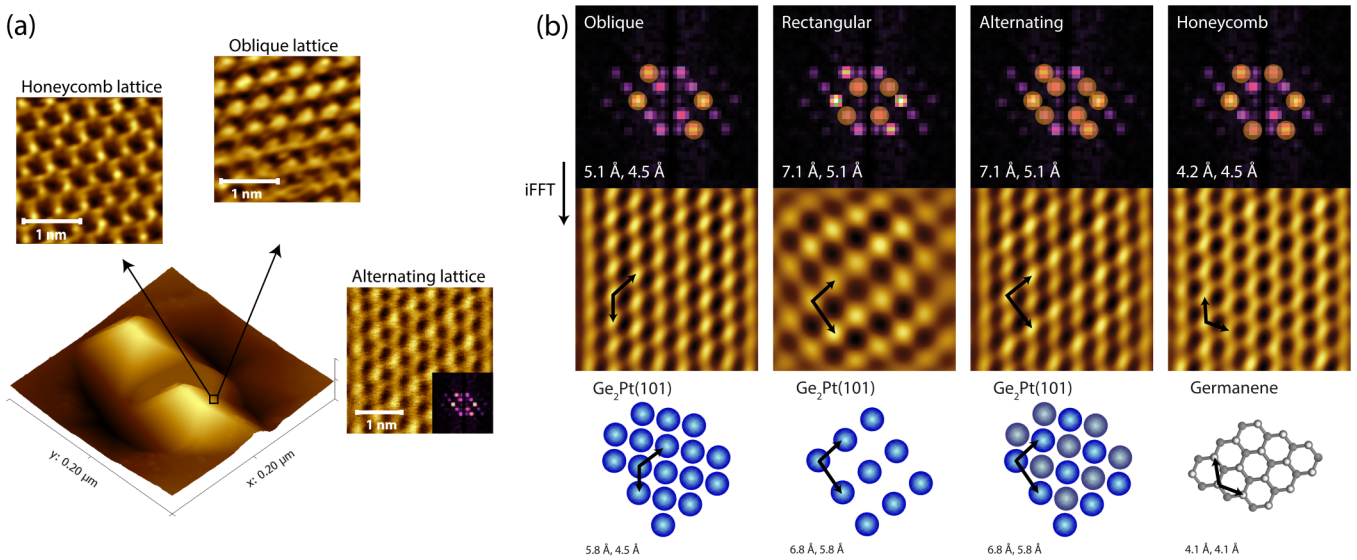

FIG. 4. (a) 3D representation of an STM topography image of two Ge_2Pt hut clusters. On the long side of the cluster, the honeycomb and oblique lattice were measured within 5 minutes of each other ($V = -1$ V; $I = 1$ nA). The alternating lattice was measured on a similar cluster ($V = -1$ V; $I = 0.5$ nA). Its inset shows the corresponding FFT. (b) In the first row, the Fourier transform of the alternating lattice is shown with four different masks that are used for the iFFT. The second row shows the corresponding iFFT topographs of the masked areas. In the last row, the corresponding atomic models of the periodic lattices are shown. For the Ge_2Pt lattices, only the Pt atoms are shown.

The system is most likely to lock in along the crystal direction with the highest corrugation, i.e., perpendicular to the zigzag rows. Here, the lattice match is almost perfect with a mismatch of only 1.8%. Along the $[1\bar{1}0]$ direction, the corrugation of the Ge substrate is much smaller. In this direction, the system is almost commensurate with a lattice mismatch of 3%. The unit cell area ratio is off unity by only 1.5%. Overall, the match is almost perfect.

B. Germanene termination on facets

In Sec. III A, we have described how the Ge_2Pt clusters grow on the Ge(110) substrate and that the long side of the clusters is terminated by {101} planes. Using STM measurements of these facets, it should be possible to verify if the atomic positions match with the expected {101} plane of the bulk crystal. Furthermore, we expect to find the germanene termination layer on these clusters in accordance to previous work.[14] Using our knowledge of the Ge_2Pt cluster, we can then determine how the germanene layer grows on the cluster.

In Fig. 4(a), an STM topograph of a double hut cluster is shown. When scanning the long side of such a hut cluster, we regularly find either a honeycomb lattice or an oblique lattice as shown in the figure. A third lattice that is regularly found on the facets of the hut clusters is a rectangular lattice with alternating brighter and darker rows as was also found previously.[14] We name this lattice the "alternating lattice." This third lattice is shown to the right of the cluster.

We found that both the oblique and the alternating lattices match the Pt atoms in the $Ge_2Pt(101)$ plane, albeit with a small difference in contrast. This confirms that the wedge clusters are terminated by {101} planes. The honeycomb lattice is attributed to the germanene layer in line with a previous work.[14] An important characteristic is that the honeycomb lattice consists of two hexagonal sub-lattices. One sub-lattice is vertically displaced with respect to the other as was predicted for free-standing germanene.[2] The honeycomb and oblique lattices that are shown were measured within 5 minutes of each other without any change to the scanning parameters. This shows that, probably due to a small tip change, the tip can become more sensitive to a particular lattice. This is in agreement with previous results where it was shown that the measured structure on these clusters is very sensitive to tunneling conditions such as the bias voltage.[14]

It can even be demonstrated that all three lattices (honeycomb, oblique, and alternating) are always captured simultaneously, because all lattices are distinguishable in the FFT. The tunneling conditions then determine the lattice that will dominate the topography image. This can most easily be seen when comparing the images in the reciprocal space. The inset of Fig. 4(a) shows the FFT of the alternating lattice. In Fig. 4(b), different sets of peaks are selected and are transformed back to real space using the inverse fast Fourier transform (iFFT). The oblique lattice can be found when taking the iFFT of the four brightest peaks as indicated in the left column. A rectangular lattice is found when taking the iFFT of the four spots closest to the origin as shown in the second column. This rectangular lattice is the same lattice as the alternating lattice which is obtained by the peaks shown in the third column. Here the same rectangular lattice is found with a second atom in the center of the rectangle. From these models, it can be seen that also the oblique and alternating lattices are very similar. The difference is that for the alternating lattice, one of the two Pt atoms in the unit cell has a different contrast. From the unit cell of Ge_2Pt, it can be seen that the Pt atoms of the $Ge_2Pt(101)$ plane all lie in the same plane. However, there are two inequivalent Pt atoms in the plane. This difference between the two Pt atoms is indicated in the model of the alternating lattice by a color contrast. This contrast exactly

matches the alternating bright and dark rows seen in the STM topography images and would thus explain the small difference between the measured oblique and alternating lattices.

The last column shows the iFFT image of the six outer reciprocal spots. This results in the honeycomb lattice. The honeycomb originates from the germanene layer that has been grown on top of the $Ge_2Pt(101)$ facet.[14] The germanene honeycomb lattice is commensurate with the Ge_2Pt oblique lattice.

It is noted that the $Ge_2Pt\{101\}$ and $Ge_2Pt\{011\}$ planes are very similar. They both have a centered rectangular unit cell albeit with slightly different lattice parameters: 6.8 Å and 5.8 Å for the {101} plane and 6.5 Å and 6.2 Å for the {011} plane. It should then not be surprising if similar results are found for the $Ge_2Pt(011)$ facets.

IV. CONCLUSION

In this work, we have shown that Ge_2Pt clusters form on the Ge(110) surface when cooling eutectic droplets down to room temperature. Germanene grows on the {101} and {011} facets of the Ge_2Pt hut clusters. Topography scans of these facets appear as one of three lattices: honeycomb, oblique, or alternating. The honeycomb is attributed to the germanene termination layer. The oblique lattice and alternating lattices originate from the underlying Ge_2Pt cluster. The germanene layer that grows on top has been found to be commensurate with the underlying Ge_2Pt substrate.

SUPPLEMENTARY MATERIAL

See supplementary material for EDX data, Ge_2Pt crystal structure, tail formation, and Ge(100) pit formation.

ACKNOWLEDGMENTS

R.v.B., P.B., and H.J.W.Z. thank the Dutch Organization for Scientific Research (NWO) for financial support (FV157 14TWDO07). J.A. and C.T. thank the DFG for financial support (Te386/12-1).

[1]K. Takeda and K. Shiraishi, Phys. Rev. B **50**, 14916 (1994).
[2]S. Cahangirov, M. Topsakal, E. Aktürk, H. Şahin, and S. Ciraci, Phys. Rev. Lett. **102**, 236804 (2009).
[3]J. C. Garcia, D. B. de Lima, L. V. C. Assali, and J. F. Justo, J. Phys. Chem. C **115**, 13242 (2011).
[4]L. C. Lew Yan Voon, E. Sandberg, R. S. Aga, and A. A. Farajian, Appl. Phys. Lett. **97**, 163114 (2010).
[5]C.-C. Liu, W. Feng, and Y. Yao, Phys. Rev. Lett. **107**, 076802 (2011).
[6]A. Acun, L. Zhang, P. Bampoulis, M. Farmanbar, A. v. Houselt, A. N. Rudenko, M. Lingenfelder, G. Brocks, B. Poelsema, M. I. Katsnelson, and H. J. W. Zandvliet, J. Phys. Condens. Matter **27**, 443002 (2015).
[7]Z. Ni, Q. Liu, K. Tang, J. Zheng, J. Zhou, R. Qin, Z. Gao, D. Yu, and J. Lu, Nano Lett. **12**, 113 (2012).
[8]M. Ezawa, J. Phys. Soc. Jpn. **84**, 121003 (2015).
[9]A. H. Bayani, D. Dideban, M. Vali, and N. Moezi, Semicond. Sci. Technol. **31**, 045009 (2016).
[10]L. Li, S.-Z. Lu, J. Pan, Z. Qin, Y.-Q. Wang, Y. Wang, G.-Y. Cao, S. Du, and H.-J. Gao, Adv. Mater. **26**, 4820 (2014).
[11]M. E. Dávila, L. Xian, S. Cahangirov, A. Rubio, and G. L. Lay, New J. Phys. **16**, 095002 (2014).
[12]M. Derivaz, D. Dentel, R. Stephan, M.-C. Hanf, A. Mehdaoui, P. Sonnet, and C. Pirri, Nano Lett. **15**, 2510 (2015).
[13]L. Zhang, P. Bampoulis, A. N. Rudenko, Q. Yao, A. van Houselt, B. Poelsema, M. I. Katsnelson, and H. J. W. Zandvliet, Phys. Rev. Lett. **116**, 256804 (2016).
[14]P. Bampoulis, L. Zhang, A. Safaei, R. v. Gastel, B. Poelsema, and H. J. W. Zandvliet, J. Phys. Condens. Matter **26**, 442001 (2014).
[15]L. Zhang, P. Bampoulis, A. v. Houselt, and H. J. W. Zandvliet, Appl. Phys. Lett. **107**, 111605 (2015).
[16]C. Volders, E. Monazami, G. Ramalingam, and P. Reinke, Nano Lett. **17**, 299 (2017).
[17]Y.-W. Mo, D. E. Savage, B. S. Swartzentruber, and M. G. Lagally, Phys. Rev. Lett. **65**, 1020 (1990).
[18]C. Teichert, Phys. Rep. **365**, 335 (2002).
[19]M. Horn-von Hoegen, B. H. Müller, T. Grabosch, and P. Kury, Phys. Rev. B **70**, 235313 (2004).
[20]I. Goldfarb, P. T. Hayden, J. H. G. Owen, and G. A. D. Briggs, Phys. Rev. Lett. **78**, 3959 (1997).
[21]P. Bampoulis, A. Acun, L. Zhang, and H. J. W. Zandvliet, Surf. Sci. **626**, 1 (2014).
[22]H. Okamoto, J. Phase Equilib. **13**, 413 (1992).
[23]L. Zhang, P. Bampoulis, A. Safaei, H. Zandvliet, and A. van Houselt, Appl. Surf. Sci. **387**, 766 (2016).
[24]G. Nolze and R. Hielscher, J. Appl. Crystallogr. **49**, 1786 (2016).
[25]K. Momma and F. Izumi, J. Appl. Crystallogr. **44**, 1272 (2011).
[26]See http://www.jmol.org/ for "Jmol: an open-source Java viewer for chemical structures in 3d with features for chemicals, crystals, materials and biomolecules" (2009).
[27]D. Nečas and P. Klapetek, Cent. Eur. J. Phys. **10**, 181 (2012).
[28]K. Schubert, S. Bhan, M. Balk, H. Breimer, E. Stolz, and P. Esslinger, "Einige strukturelle Ergebnisse an metallischen Phasen. IV," Naturwissenschaften **46**, 647 (1959).
[29]L. V. Arapkina and V. A. Yuryev, Physics-Uspekhi **53**, 279 (2010).
[30]H. Wang and T. Wu, Nanoscale Res. Lett. **7**, 110 (2012).
[31]S. Jung Jung, T. Lutz, and J. J. Boland, J. Vac. Sci. Technol. A Vac. Surf. Films **29**, 051403 (2011).
[32]S. Curiotto, F. Leroy, F. Cheynis, and P. Müller, Nano. Lett. **15**, 4788 (2015).
[33]P. Sutter, P. A. Bennett, J. I. Flege, and E. Sutter, Phys. Rev. Lett. **99**, 125504 (2007).
[34]S. J. Rathi, D. J. Smith, and J. Drucker, Nano Lett. **13**, 3878 (2013).
[35]R. C. Ellis, J. Appl. Phys. **25**, 1497 (1954).
[36]P. R. Camp, J. Electrochem. Soc. **102**, 586 (1955).
[37]B. R. Jany, N. Gauquelin, T. Willhammar, M. Nikiel, K. H. W. V. D. Bos, A. Janas, K. Szajna, J. Verbeeck, S. V. Aert, G. V. Tendeloo, and F. Krok, Sci. Rep. **7**, 42420 (2017).